

**dc photoconduction studies of single-walled carbon nanotube bundles**

D. Chowdhary and N. A. Kouklin\*

*Department of Electrical Engineering and Computer Science, University of Wisconsin–Milwaukee, Milwaukee, Wisconsin 53201, USA*

(Received 19 March 2007; published 16 July 2007)

The effect of marked photoconduction in  $\sim 30$  nm diameter controllably engineered nanotube bundles is observed and investigated by a series of Raman-dc-photoconduction and light absorption measurements. The photocurrent in the bundle is found to change nearly linearly with applied bias and light intensity, attributed to free carrier photogeneration in individual semiconducting tubes. The primary mechanism of photoexcitation is a resonant electron-hole excitation, assigned to  $v2 \rightarrow c2$  type. Photocurrent characteristics are observed to evolve from non-Ohmic to Ohmic-like with increasing excitation powers, and the results are discussed within the model of heterogeneous conduction, proposed earlier.

DOI: [10.1103/PhysRevB.76.035416](https://doi.org/10.1103/PhysRevB.76.035416)

PACS number(s): 73.50.Pz, 73.63.Fg

First discovered by Ijima, carbon nanotubes<sup>1</sup> (CNs) have unique electronic and optical properties, and continue to be a subject of intense scientific research and investigation. A class of single-walled nanotubes (SWNTs) is of particular interest because they exhibit a number of functionalities that do not exist in other material systems. At the same time, SWNT also can be semiconducting and metallic depending on their chirality. A critical aspect of semiconductor materials lies in their strong sensitivity to optical radiation; however, the paradigm has not yet been fully investigated for CN.

In contrast to bulk materials, the electronic properties of low dimensional structures, including semiconductor quantum dots, wires, and SWNTs, are strongly size dependent. Owing to a large variance in the structural parameters and the lack of techniques to reliably sort SWNTs by their type and chirality, any experimental and theoretical investigation of optoelectrical characteristics of SWNTs becomes quite challenging. The problem can be addressed by simultaneously acquiring Raman and photocurrent signals, which allows one to concurrently probe and thus correlate the geometric and photoelectrical properties of the nanotubes. The approach can serve as a convenient vehicle to experimentally study optoelectrical phenomena in highly complex electronic media, such as SWNTs; the latter predominantly exist in the state of small bundles.

Light interaction with individual and noninteracting nanotubes has been theoretically shown to exhibit a strong resonant-dependent behavior commensurate with the nanotube density of state and periodic boundary conditions, also known as Van Hove singularities. Bachilo *et al.* were the first to successfully obtain emission and/or absorption spectra and excitation-emission matrix from the surfactant-modified and presumably individual semiconducting nanotubes, with the results to have been in accordance with the line of theoretical predictions.<sup>2</sup> The authors have also pointed to the presence of strong quenching of light emission from nanotube bundles, the formation of which is self-regulated and favored by short-range van der Waals forces. A strong sidewall attraction induced by interatomic forces and  $\pi$ -stacking interactions<sup>3–5</sup> can generally lead to a new optoelectronic response, largely influenced by a degree of intertube electronic coupling and transport. When excited with light, semiconducting tubes become highly conductive, which will expectedly lead to in-

creased coupling between the neighboring components. As a result, the electronic wave function can extend well over several tubes and the quenching effect, thus, can be attributed to a fast nonradiative transfer of energy from semiconducting to metallic tubes.

Photoinduced energy transfer has been long known to play an important role as it governs many optical characteristics of low dimensional systems with strong electronic coupling and can also be exploited in near field imaging applications.<sup>6</sup> As for nanotubes, the property also poses an important question to the mechanism of the photoconduction of the SWNT bundles. From the standpoint of the results reported in Ref. 2, a strong localization of the excitations on isolated metallic components (the metallic content is estimated to be of  $\sim 30\%$ ) will expectedly affect (facilitate) intertube electronic transport as being overall mediated by carrier hopping, but mostly indirectly; therefore, the induced photocurrent will only constitute a second order effect. In this study, we show that  $\sim 30$  nm diameter SWNT bundles exhibit a marked photoresponse that deviates substantially from the scenario described above and instead is attributed to resonance photoexcitation and transport of photogenerated carriers in semiconducting components as a dominant photoconduction mechanism. The effects of photoconduction in nanotube samples have been recently observed by several authors.<sup>7–11</sup> The reports generally point to dissimilar mechanisms underlying CN photoconduction phenomena. For instance, in individual semiconducting tubes configured as field-effect transistors, the photocurrent measured using lock-in techniques has shown a linear change with light intensity.<sup>8</sup> Yet, in nanotube suspensions, a sublinear response was observed and attributed to a bimolecular recombination.<sup>7</sup> At the same time, a linear dependence was observed for thin films of carbon nanotubes, while a saturation of the photocurrent signal at larger excitation powers has been tentatively prescribed to a slow replenishment of the carriers.<sup>9</sup> The controversy generally implies a highly intricate picture of physical mechanisms underlying light-nanotube interaction and photoconduction phenomena. At the same time, the difference in the reported results can also be a result of extrinsic dependences such as variation in sample processing routes, unaccounted electromechanical effects, substrate contribution, and light induced heating.

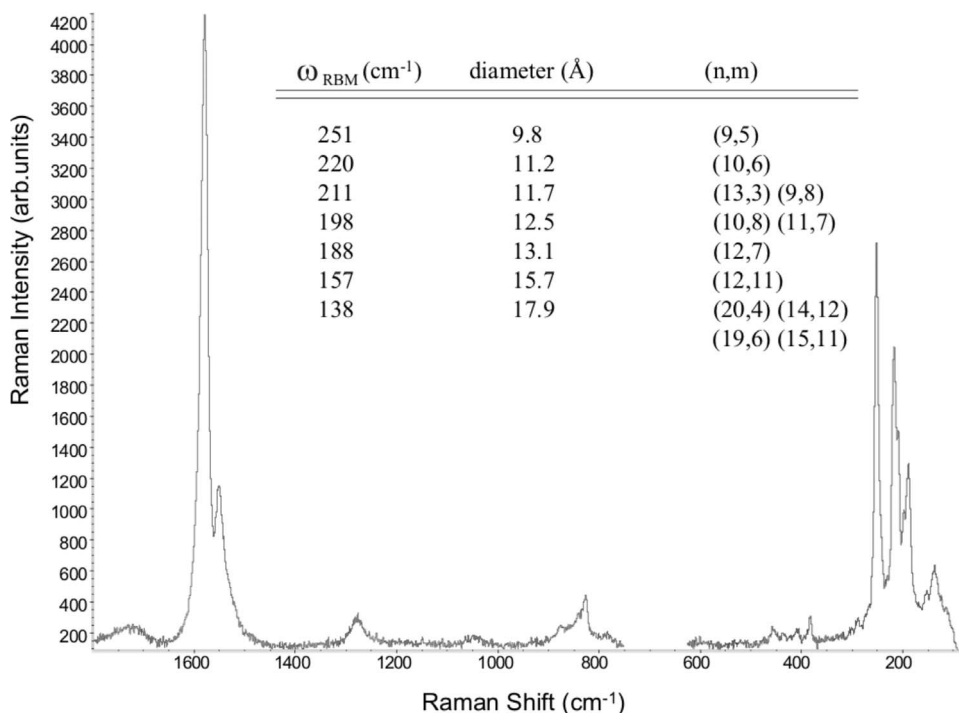


FIG. 1. Raman scattering spectrum of nanotubes comprising the bundles excited with  $\sim 785$  nm laser line. The inset lists the average diameter and the closest  $n$ - $m$  numbers of nanotubes assigned according to their RBM frequencies. No metallic tubes are resonantly excited under the experimental conditions as clarified by Fig. 2.

In this work, the effect of photoconduction has been systematically studied based on the model of aligned, close-packed, and inclusion-free single-walled nanotube bundles. To minimize any variation in the structural characteristics of the bundle and to avoid any substrate influence (via field gating effect), air suspended bundles were prepared by a refined dielectrophoretic technique.<sup>13</sup> The technique offers an excellent command over bundle structural characteristics and provides a simple method to controllably position resultant bundles onto support electrodes with a strong adhesion and Ohmic contacts.<sup>13</sup> Small (i.e.,  $<100$  nm) diameter bundles featuring a close-packed, parallel, and void-free arrangement of CNs are found to consistently exhibit a strong photoconduction response (with at least 17 devices tested) that changes almost linearly with incident light intensity, typical of conventional semiconductors. With the help of Raman experiments, we also conclude that the primary mechanism of photoexcitation is a resonant free carrier generation in individual semiconducting tubes prescribed to  $v_2 \rightarrow c_2$  transitions, as discussed further.

Purified and highly crystalline HiPco® single-walled nanotubes used were obtained from Carbon Nanotechnologies and have diameters of  $\sim 0.7$ – $1.3$  nm and the energy band gap of  $\sim 0.8$ – $1.3$  eV. To assemble aligned  $\sim 30$  nm diameter and  $\sim 20$ – $40$   $\mu\text{m}$  long CN bundles, the nanotubes were first suspended uniformly in chloroform by rigorous sonication for several hours, while a 5 V peak-to-peak ac electric field was applied to direct the assembly of the bundles across the gap formed by oppositely aligned tungsten microelectrodes; further details on the assembly can be found elsewhere.<sup>13</sup>

The photoconduction experiments have been accomplished using a Raman spectrometer operating in conjunction with an Olympus B51 optical microscope. Stokes part of SWNT Raman spectra was collected to probe for *nanotube*

*specific* excitation processes, while anti-Stokes part of  $G$  band has been used, in addition, to monitor the absolute temperature of the samples. Since both the Raman scattering and photoconduction effect show a strong resonant-dependent behavior, the photoconduction is to be particularly dominated by the tubes with the strongest Raman active radial breathing modes (RBMs), given that a nonresonant absorption cross section decays fast with an inverse square of the photon energy.<sup>14</sup> This strong resonant-dependent behavior provides a simple way to quickly and reliably identify nanotube-specific light absorption processes.

Raman scattering data were obtained using a wavelength-dispersive Raman spectrometer (Thermo-Nicolet) operating in the backscattering configuration. The samples were illuminated with a 785 nm laser line, and the collected light was analyzed with a thermoelectrically cooled InGaAs detector. The results of Raman measurements are presented in Fig. 1. As one can clearly see, the spectrum is dominated by a narrow  $G$  band with a peak position at  $\sim 1600$   $\text{cm}^{-1}$ , while  $D$  band is also present, its intensity is much smaller, suggestive of overall high crystal quality of the nanotube samples. Small intensity RBM bands can be further found at the lower-frequency part of the spectrum. Based on the direct assignment rule,<sup>15</sup> structural characteristics, i.e.,  $n$ - $m$  numbers of photoexcited CNs, were identified according to their RBM peaks, with the details listed in the inset of Fig. 1. The intersection of 1.57 eV (785 nm) line with the dipole allowed transition curves, known as Kataura plot (Fig. 2), gives two possible resonant transition regions, which are marked by circles (this accounts for the inaccuracy in the transition diameter of  $\sim 0.2$  nm). While it has been recently found that the Kataura plot gives somewhat incorrect optical transition energies for smaller nanotube diameters, the inaccuracy is marginal for  $E_{22}^S$  and  $E_{11}^M$  transitions for excitation powers of 1.57 eV and the range of diameters  $<1.3$  nm.<sup>16</sup>

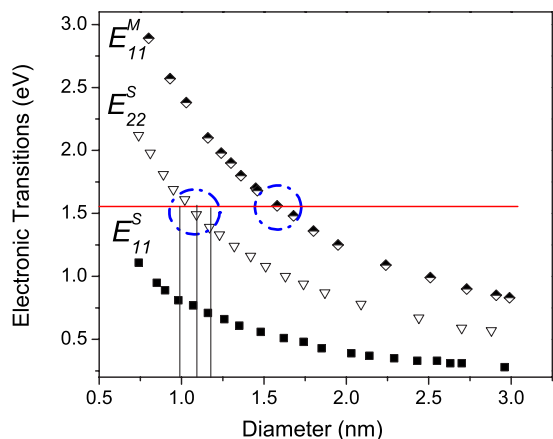


FIG. 2. (Color online) Electronic transitions plotted as a function of nanotube diameter after Ref. 12. The circles show possible transitions that are in resonance with incoming radiation and assigned to (9, 5), (10, 6), (13, 3), and (9, 8) (chiral semiconducting) tubes.

Among all semiconducting tubes listed in the inset of Fig. 1, only those having diameters of 0.98, 1.12, and 1.17 nm can be resonantly excited, while their RBM peaks also dominate the low-frequency part of the Raman spectrum. In terms of the  $n$  and  $m$  numbers, we find that (9,5), (10,6), (13,3), and (9,8) tubes, all of which are S2 type ( $[2n+m] \bmod 3 = 2$ ), will experience resonance excitation, while the allowed transitions are prescribed to  $v_2 \rightarrow c_2$  type, marked as  $E_{22}^S$ . The RBM intensities of these tubes vary depending on their diameter and chirality. Since the tubes have somewhat similar diameters, the main variation of the RBM intensities comes from the chirality dependence. Using the results of previous calculations,<sup>16</sup> we estimate that at least half of the total number of resonantly excited SWNTs will be (9,5) ones.

Figure 3 illustrates the results of light transmittance measurements carried out similarly on solution suspended

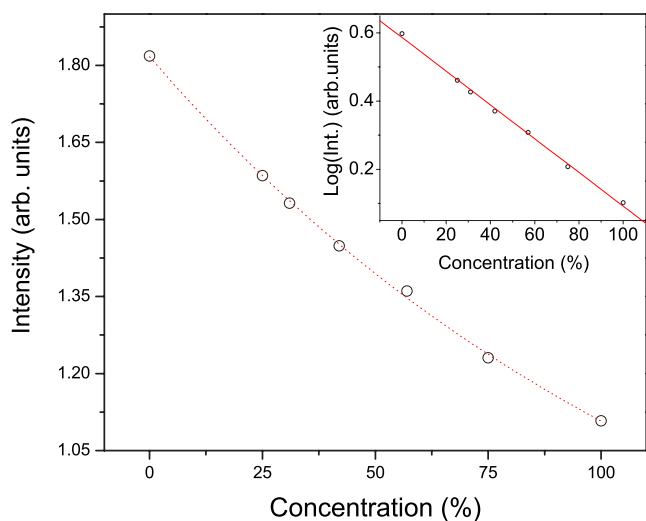


FIG. 3. (Color online) Intensity vs concentration measurements. The inset (logarithmic plot) reveals a clear exponential dependence of the intensity characteristics.

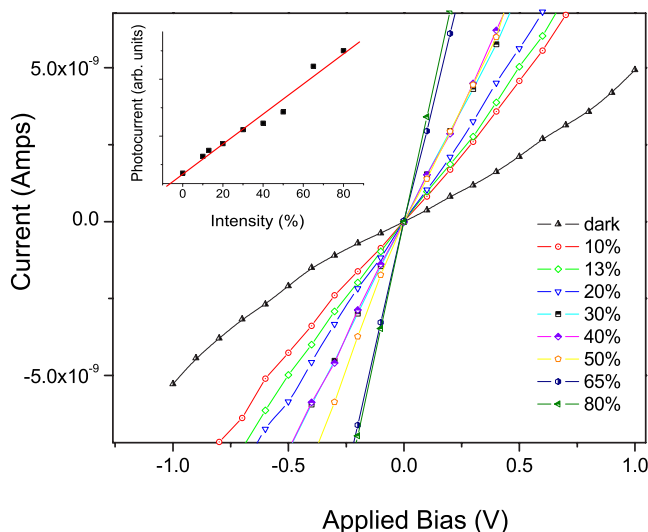


FIG. 4. (Color online) Intensity dependent current-voltage ( $I$ - $V$ ) characteristics obtained under different illumination conditions. The samples are excited with a focused 785 nm laser beam. The excitation spot is of 15  $\mu\text{m}$  diameter, with 10% illumination power corresponding to  $\sim 10$  mW. The inset shows a current vs intensity curve obtained at an applied bias of 0.8 V.

SWNTs as a function of their concentration, which was controlled by a dilution method. The results show that the light intensity falls off quickly with the nanotube concentration, which points to the presence of a strong light attenuation by the nanotube solutions. Plotted on a semilogarithmic scale, the data appear as a straight line (Fig. 3, inset), confirming that the attenuation is primarily induced by absorption of light by semiconducting nanotubes.

Figure 4 shows the results of intensity-dependent photocurrent measurements that reveal nearly a tenfold increase in the current in the bundles subjected to laser radiation. The photocurrent changes linearly with intensity (Fig. 4, inset). At the same time, while a strong increase in the temperature of the samples (calculated based on the Stokes and anti-Stokes intensity ratios of  $G$  band<sup>17</sup>) can be registered (Fig. 5, inset), no saturation of the signal has been observed, implying that direct resonance excitation rather than electron-phonon scattering processes control the response.

Current-voltage characteristics obtained as a function of the incident light intensity clearly exhibit a gradual reversal from being slightly nonmetallic to metallic with increased excitation powers (Fig. 4). Non-Ohmic response can be explained by several factors, including the contribution of contacts, the presence of defects, or localization effects. We also have performed a set of similar transport measurements on other nanotube assemblies, including random CN networks and less ordered bundles. The results consistently revealed an Ohmic-type conductance for such CN samples, which requires us to exclude contacts and nanotube defects as the possible origin of the effect. The behavior is very consistent with the results of independently performed transport studies by others, in which observed nonmetallic conductance has been attributed primarily to either intrinsic characteristics of the bundles<sup>18</sup> or individual semiconducting nanotubes.<sup>19</sup>

To better understand the nonmetallic response observed,

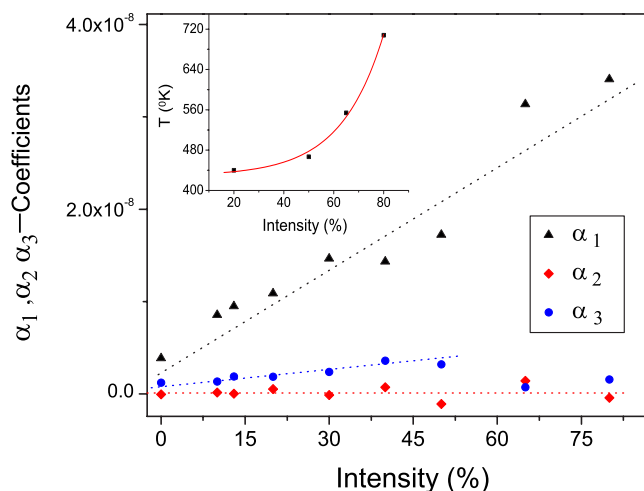


FIG. 5. (Color online) Plots as a function of light intensity,  $\alpha_1$ ,  $\alpha_2$ , and  $\alpha_3$  coefficients obtained by fitting photo  $I$ - $V$ 's. The inset shows sample temperature as a function of incident intensity fitted by exponential dependence (solid line).

the photocurrent-voltage ( $I$ - $V$ ) data were readily fitted with  $I = \alpha_1 V + \alpha_2 V^2 + \alpha_3 V^3$  (Fig. 5), with  $\alpha_1, \alpha_3 > 0$ . Furthermore, as  $\alpha_2 \approx 0$ , we confirm that no rectification is present in our device (i.e., no change in current values are present upon the reversal of the bias). Given that there is no *a priori* reason to believe in the absolute equivalence of the left and right contacts, this indirectly proves that the contact resistance is negligible and the observed photoeffect is entirely due to the bundle. According to Fig. 5,  $\alpha_1$  (linear term) grows monotonically with intensity over the whole range of incident powers, while  $\alpha_3$  (third order term) exhibits a linear change only at lower excitation powers. A strong relative decline of  $\alpha_3$  is observed to start at the intensity of  $\sim 50\%$ .

Transport in SWNT bundles has been previously found to exhibit intermix behaviors with metallic-nonmetallic conductance reversibility, determined by a change in the sign of conductance-temperature derivative, i.e.,  $d\sigma/dT$  at a cross-over temperature  $T^*$ .<sup>18</sup> An intensity value of  $\sim 50\%$  exactly coincides with the onset of a strong temperature increase in the bundle, which directly indicates a thermally activated linear transport taking place in the bundles. While  $T^*$  was reported to lie in the range of 35–250 K,<sup>18</sup> the non-Ohmic/Ohmic reversal of photo- $I$ - $V$ 's takes place at a much higher  $T$  of  $\sim 450$  K (corresponding to  $\sim 50\%$  intensity). The discrepancy is likely associated with the fact that the optical method employed here provides for more accurate monitoring of the absolute temperature of the samples compared to that accomplished with the use of  $T$  sensor, since the latter simply fails to account for any current induced heating effects that can be substantial.

The mechanism for nonmetallic transport is generally recognized as a variable-range hopping conductance.<sup>20</sup> For the range of  $T > T^*$ , one would highly anticipate to observe a metalliclike response along with a gradual increase in the sample resistance at increased excitation powers if the photoeffect were simply due to heating. In contrast, a substantial

increase in the sample conductance has been observed and taken as evidence of light induced free carrier generation in individual nanotubes; the latter can be readily analyzed by relating a current change  $\Delta i$  to that of conductance,  $\Delta\sigma$ . For a nearly linear transport regime, one can obtain the following expression:

$$\begin{aligned} \Delta i(I, T, V) &\approx \Delta\sigma(I, T, V)V \propto \Delta n(I)\mu(T)V \\ &\propto \Delta n(I)[\mu_0(T) + \mu_1(T)V + \mu_2(T)V^2]V, \end{aligned}$$

where  $\mu_0, \mu_1, \mu_2$  are the mobility voltage prefactors, while the photogenerated excess free carrier density  $\Delta n$  is assumed to mainly depend on photogeneration rate  $G$ , i.e., proportional to the intensity of light  $I$ :  $\Delta n \propto G \propto I$ . This assumption fits well into the picture of the photoconduction behavior observed and discussed thus far. In particular, as  $\alpha_{1,2,3} \propto \Delta n(I)\mu_{0,1,2}(T)$ ,  $\alpha_1$  and  $\alpha_3$  are anticipated to show a linear change with light intensity for low incident powers (and temperatures), in absolute agreement with the experimental findings (Fig. 5).

The key outcome of the above formula is that it allows one to easily deconvolve the effects of heating and carrier photogeneration concurrently taking place in nanotube bundles and affecting two different physical parameters: carrier mobility and density. Since at high temperatures hopping is no longer a limiting transport mechanism, the response is determined primarily by intrinsic characteristics of semiconducting and metallic tubes. Since the resistivity of metallic SWNTs scales up linearly with the temperature<sup>21</sup> and thus exponentially with intensity in our case, the amount of current carried by the metallic components will also be exponentially reduced. In parallel, as the density of photogenerated carriers increases with both intensity and temperature, semiconducting tubes will show significantly less resistance with increased excitation powers. On the other hand, thermal excitations are expected to compete only weakly with direct resonant excitation processes since  $kT \ll E_{gap}$ , thereby explaining why the observed dependence is not exponential with inverse temperature but linear with intensity. As a final remark, as the optical excitations in individual nanotubes are excitonic by nature<sup>22–24</sup> and given that we could easily obtain a photocurrent signal at biases of  $\sim 1$  mV  $\ll$  exciton binding energy ( $\sim 0.2$ – $0.4$  eV  $\gg kT$ ), the mechanism of free carrier formation is likely to be exciton-exciton rather than field assisted annihilation.

For a complete description of the photoconduction phenomenon in CN bundles, the question on the photoconduction in resonantly excited metallic tubes remains to be addressed. It is likely that the response will be dominated particularly by light heating effects and will affect mainly the carrier mobility characteristics of nanotube samples; however, in view of possible nonresonant and resonant energy transfers to other nanotubes, a detailed investigation of this question is needed and therefore postponed until future work.

One of the authors thanks S. Sen for his assistance with part of the experimental measurements. The work was supported by NSF Grant No. ECCS 0621919.

\*nkouklin@uwm.edu

- <sup>1</sup>S. Iijima, *Nature (London)* **354**, 56 (1991).
- <sup>2</sup>S. M. Bachilo, M. S. Strano, C. Kittrell, R. H. Hauge, R. E. Smalley, and A. R. B. Weisman, *Science* **298**, 2361 (2002).
- <sup>3</sup>I. V. Bondarev and P. Lambin, *Phys. Rev. B* **72**, 035451 (2005).
- <sup>4</sup>C.-H. Sun, G.-Q. Lu, and H.-M. Cheng, *Phys. Rev. B* **73**, 195414 (2006).
- <sup>5</sup>F. Tournus, S. Latil, M. I. Heggie, and J. C. Charlier, *Phys. Rev. B* **72**, 075431 (2005).
- <sup>6</sup>G. Colas des Francs, C. Girard, and O. J. F. Martin, *Phys. Rev. A* **67**, 053805 (2003).
- <sup>7</sup>J. C. Bunning, K. J. Donovan, K. Scott, and M. Somerton, *Phys. Rev. B* **71**, 085412 (2005).
- <sup>8</sup>M. Freitag, Y. Martin, J. A. Misewich, R. Martel, and P. Avouris, *Nano Lett.* **3**, 1067 (2003).
- <sup>9</sup>A. Fujiwara, Y. Matsuoka, H. Suematsu, H. Kataura, and Y. Achiba, *Jpn. J. Appl. Phys., Part 2* **40**, L1229 (2001).
- <sup>10</sup>D. A. Stewart and F. Léonard, *Phys. Rev. Lett.* **93**, 107401 (2004).
- <sup>11</sup>Y. Zhang and S. Iijima, *Phys. Rev. Lett.* **82**, 3472 (1999).
- <sup>12</sup>A. Jorio, A. G. Souza Filho, G. Dresselhaus, M. S. Dresselhaus, A. K. Swan, M. S. Ünlü, B. B. Goldberg, M. A. Pimenta, J. H. Hafner, C. M. Lieber, and R. Saito, *Phys. Rev. B* **65**, 155412 (2002).
- <sup>13</sup>N. Kouklin, W. Kim, A. Lazareck, and J. Xu, *Appl. Phys. Lett.* **87**, 173901 (2005).
- <sup>14</sup>E. Malic, M. Hirtschulz, F. Milde, A. Knorr, and S. Reich, *Phys. Rev. B* **74**, 195431 (2006).
- <sup>15</sup>A. Jorio, R. Saito, J. H. Hafner, C. M. Lieber, M. Hunter, T. McClure, G. Dresselhaus, and M. S. Dresselhaus, *Phys. Rev. Lett.* **86**, 1118 (2001).
- <sup>16</sup>A. Jorio, C. Fantini, M. A. Pimenta, R. B. Capaz, G. G. Samsonidze, G. Dresselhaus, M. S. Dresselhaus, J. Jiang, N. Kobayashi, A. Grüneis, and R. Saito, *Phys. Rev. B* **71**, 075401 (2005).
- <sup>17</sup>W. Tang, H. Rosen, P. Buchmann, P. Vettiger, and D. Webb, *J. Appl. Phys.* **68**, 5930 (1990).
- <sup>18</sup>A. B. Kaiser, G. Düsberg, and S. Roth, *Phys. Rev. B* **57**, 1418 (1998).
- <sup>19</sup>V. Skákalová, A. B. Kaiser, Y. S. Woo, and S. Roth, *Phys. Rev. B* **74**, 085403 (2006).
- <sup>20</sup>G. T. Kim, E. S. Choi, D. C. Kim, D. S. Suh, Y. W. Park, K. Liu, G. Duesberg, and S. Roth, *Phys. Rev. B* **58**, 16064 (1998).
- <sup>21</sup>C. L. Kane, E. J. Mele, R. S. Lee, J. E. Fischer, P. Petit, H. Dai, A. Thess, R. E. Smalley, A. R. Verschuere, S. J. Tans, and C. Dekker, *Europhys. Lett.* **43**, 683 (1998).
- <sup>22</sup>L. Marty, E. Adam, L. Albert, R. Doyon, D. Ménard, and R. Martel, *Phys. Rev. Lett.* **96**, 136803 (2006).
- <sup>23</sup>S. Uryu and T. Ando, *Phys. Rev. B* **74**, 155411 (2006).
- <sup>24</sup>Z. Wang, H. Pedrosa, T. Krauss, and L. Rothberg, *Phys. Rev. Lett.* **96**, 047403 (2006).